Research Square

Preprints are preliminary reports that have not undergone peer review.
They should not be considered conclusive, used to inform clinical practice,
or referenced by the media as validated information.

Optimising Diaphragmatic Navigation and Radial Sampling Percentage in Free-Breathing Liver 3D VANE MRI: A Prospective Intra-Subject Study

□□ □
he Second Affiliated Hospital of Dalian Medical University
Boyun Yan
he Second Affiliated Hospital of Dalian Medical University
Huicong Shen
he Second Affiliated Hospital of Dalian Medical University
Zhaoying Liu
he Second Affiliated Hospital of Dalian Medical University
Jiuming Fu
he Second Affiliated Hospital of Dalian Medical University
Liu Ya jie
liuyajie40@163.com
he Second Affiliated Hospital of Dalian Medical University
Yongkun Kang
he Second Affiliated Hospital of Dalian Medical University

Research Article

Keywords: Liver MRI, Free-breathing MRI, 3D VANE, Diaphragmatic navigation, Radial sampling

Posted Date: June 5th, 2026

DOI: https://doi.org/10.21203/rs.3.rs-9816794/v1

License: This work is licensed under a Creative Commons Attribution 4.0 International License. Read Full License

Additional Declarations: No competing interests reported.

Abstract

Objective

To evaluate the effects of diaphragmatic navigation and radial sampling fraction on image quality and scan efficiency in free-breathing liver three-dimensional volumetric navigated acquisition(3D VANE) MRI, and to identify a balanced parameter combination.

Methods

In this prospective intra-individual study, 30 subjects underwent ten free-breathing 3D VANE acquisitions using five radial sampling fractions (100%, 120%, 140%, 160%, 180%) with and withoutdiaphragmaticatic navigation. Two abdominal radiologists independently assessed subjective image quality. Objective metrics included liver signal-to-noise ratio (SNR), background noise standard deviation (SD), and lesion contrast-to-noise ratio (CNR). Objective data were analyzed using two-way repeated-measures analysis of variance(ANOVA); subjective scores were compared using Friedman and Wilcoxon signed-rank tests with correction for multiple comparisons.

Results

Both diaphragmatic navigation and radial sampling fraction significantly affected SNR, SD, and lesion CNR. Compared with non-navigation, navigation improved SNR and CNR, reduced SD, and yielded higher subjective scores. Increasing radial sampling fraction improved image quality but prolonged scan time. Under navigation conditions, the 140% group showed comparable subjective scores to the 160% and 180% groups, with a shorter scan time (211.9 ± 56.2 s vs 249.0 ± 59.4 s and 271.4 ± 93.1 s).

Conclusion

Diaphragmatic navigation and radial sampling fraction both influence image quality in free-breathing liver 3D VANE MRI. Under the conditions of this study, 140% radial sampling with navigation provides a favorable balance between image quality and scan efficiency.

1Preface

Liver MRI is crucial for detecting and characterising lesions, as well as assessing therapy[1, 2], with image quality significantly impacting lesion visibility and diagnostic confidence. Traditional three-dimensional T1-weighted imaging (3D T1WI) typically requires breath-hold acquisition to reduce respiratory motion artefacts, demanding considerable patient cooperation [3]. However, as the population ages, there is an increasing number of elderly patients, those with cardiopulmonary comorbidities, critically ill individuals, and patients with limited breath-holding capacity. This trend makes reliable breath-hold acquisitions increasingly difficult [4–6]. Poor compliance with breath-hold instructions can result in blurred images, necessitating repeated scans. Additionally, breath-holding, being a temporary and non-physiological respiratory control state, may cause fluctuations in physiological parameters [7, 8]. Consequently, optimising abdominal MRI techniques to achieve diagnostically robust images while minimising patient cooperation requirements is a crucial clinical goal.

Free-breathing imaging presents a viable solution to the challenges previously mentioned[9–14]. Unlike breath-hold techniques, free-breathing scans minimise reliance on patient cooperation, making them ideal for individuals who struggle to hold their breath or maintain a stable breath-hold. Techniques such as respiratory gating or diaphragm navigation track respiratory motion, acquiring data during stable respiratory phases. This approach reduces respiration-related artefacts and enhances the quality of abdominal MRI images [15].The Three-dimensional Volumetric Navigated Acquisition(3D VANE)method, a stack-of-stars–based free-breathing three-dimensional imaging technique, improves motion robustness by employing in-plane radial sampling and repeatedly oversampling the k-space centre [16, 17]. Nevertheless, radial free-breathing imaging can still suffer from streak and undersampling artefacts [18]. Simply increasing radial sampling might enhance image uniformity and detail but would extend scan duration and decrease acquisition efficiency [19, 20]. Thus, in free-breathing liver MRI, a systematic evaluation is necessary to strike an optimal balance between image quality and scanning efficiency.While previous research has independently explored the impacts of free-breathing radial acquisition, respiratory navigation strategies, and radial sampling fraction on image quality [13, 15, 19, 20], there is a lack of evidence regarding the joint optimisation of diaphragm navigation status and radial sampling fraction within the same subjects.

This study seeks to assess how the state of diaphragmatic navigation and the Percentageof radial sampling interactively affect subjective image quality, objective quantitative metrics, and scan time in free-breathing 3D VANE MRI of the liver. The aim is to identify parameter combinations that optimise the balance between image quality and scanning efficiency, thereby providing a foundation for enhancing free-breathing liver MRI protocols.

2 Materials and Methods

2.1 Study population

This study was a prospective, single-centre, within-subject repeated-measures investigation, approved by our hospital's Institutional Ethics Committee (No. KY2025-692-01). All participants gave written informed consent before the examination. A consecutive series of 32 subjects were enrolled. Inclusion criteria required the absence of contraindications to MRI, while exclusion criteria included the inability to complete all study sequences due to prolonged scan duration, poor positional cooperation, or similar reasons, which would prevent subsequent analyses.

2.2 Image Acquisition

All participants had upper abdominal MRI scans performed on a 3.0 T scanner (Ingenia CX 3.0T, Philips Healthcare) equipped with a 32-channel torso phased-array coil. They were positioned supine with a headfirst orientation. Initially, standard localisation scans were conducted. An axial T2-weighted sequence was then acquired for anatomical localisation and image reference. This was followed by the acquisition of a liver 3D VANE sequence during free breathing.This study utilised a within-subject, two-factor scanning design. The first factor, radial sampling percentage, was tested at five levels: 100%, 120%, 140%, 160%, and 180%. The second factor, diaphragmatic navigation status, had two levels: with and without diaphragmatic navigation. Each participant completed 10 3D VANE sequences.In the condition with diaphragmatic navigation, gating was employed for monitoring and triggering respiratory motion. The navigation position was set over the right diaphragmatic dome, and prospective gating was used to restrict data acquisition to a stable respiratory phase. In contrast, data in the no-navigation condition were collected during free breathing.All other scanning parameters remained constant: Repetition time(TR) 3.5 ms, Echo time（TE） 1.42 ms, Field of view（FOV） 450 × 450 mm², voxel size 1.5 × 1.5 × 3

mm³, slice spacing − 1.48 mm, flip angle 10°, Number of Signal Averages（NSA) 1, and fat suppression via Spectral attenuated inversion recovery(SPAIR）. Table 1 details the sequence parameter combinations and scan times for each condition. The T2-weighted imaging（T2WI） sequence served solely as an anatomical reference and was excluded from parameter comparison analyses.To minimise potential biases from acquisition order on image quality assessment, the 10 sequences were acquired in a randomised order for each subject.

2.3 Image Objective Evaluation

Images were transferred to the Philips workstation (Philips IntelliSpace Portal; Philips Healthcare) for analysis. Two abdominal MRI radiologists, blinded to the scanning parameters, conducted an objective evaluation. Upon confirming satisfactory interobserver agreement, the average of their measurements was used for further analysis.In the largest cross-section of the liver, three circular regions of interest (ROIs), each measuring 40–60 mm², were placed within the hepatic parenchyma. Care was taken to avoid intrahepatic vessels and noticeable artefact regions. The mean signal intensity (SI) of each ROI was measured, and their average was recorded as the liver signal intensity (SI_liver). Similarly, on the same slice, three ROIs were positioned in the background region behind the erector spinae muscles using the same method. The standard deviation of signal intensity for each ROI was measured, and the mean of these values was defined as the background noise standard deviation (SD_background).In cases where hepatic lesions were present, the largest lesion in each subject was selected as the target lesion. A representative ROI was delineated on its largest axial slice. For cystic lesions, ROIs avoided the margins, septations, and artefacts, while for solid lesions, areas of necrosis or haemorrhage were avoided. The mean signal intensity measured was recorded as SI_lesion. To ensure comparability of measurements, the ROI slice, location, and area were kept as consistent as possible across image sets for each subject. The liver signal-to-noise ratio (SNR) and lesion contrast-to-noise ratio (CNR) were calculated using the following formulas: [insert formulas here].

SNR = SI_liver / SD_background

CNR = |SI_lesion − SI_liver| / SD_background

2.4 Subjective Image Evaluation

Two radiologists, with 15 and 10 years of experience in interpreting abdominal MRI scans, respectively, conducted independent, blinded evaluations. They assessed seven criteria: the sharpness of liver margins, clarity of intrahepatic vasculature, presence of stripe artefacts, lesion conspicuity (only in subjects with hepatic lesions), overall image quality, effectiveness of fat suppression, and clarity of pancreatic architecture. Each criterion was rated on a 5-point scale, where higher scores denoted superior image quality and fewer artefacts. The interobserver agreement between the radiologists was evaluated. Upon achieving acceptable agreement, they conducted a joint review to establish a consensus score for further statistical analysis.

2.5 Statistical Analysis

The data analysis was conducted using SPSS version 27.0. To evaluate the normality of continuous variables, the Shapiro–Wilk test was employed. Variables that followed a normal distribution are expressed as mean ± standard deviation, while those that did not are presented as median and interquartile range. Ordinal subjective scores are reported as median (Q25, Q75).

Objective quantitative metrics were evaluated using a two-way repeated measures analysis of variance (ANOVA) to determine the effects of diaphragm navigation status, radial sampling proportion, and their interaction. Mauchly’s

test of sphericity was conducted for the radial sampling Percentageand their interaction. When the sphericity assumption was violated, the Greenhouse–Geisser correction was applied to adjust the degrees of freedom. Post hoc pairwise comparisons were adjusted for multiple testing using the Holm procedure. The analysis reported F values, corrected degrees of freedom, *P* values, and partial η^2.

Subjective image quality scores across the 10 sequence groups were analysed using the Friedman test. Upon finding statistically significant overall differences, pairwise comparisons were conducted using the Wilcoxon signed-rank test, applying Holm correction for multiple comparisons. The weighted kappa statistic assessed interobserver agreement for subjective ratings, while the intraclass correlation coefficient (ICC) evaluated the consistency of objective quantitative measurements. All tests were two-sided, with a *P*-value of less than 0.05 deemed statistically significant.

3 Results

3.1 Basic characteristics of the participants

Initially, 32 participants were enrolled in the study. However, 2 were excluded due to their inability to complete all sequence scans. Consequently, 30 participants successfully completed the acquisition of all ten 3D VANE sequence sets and were included in the analysis. Among these, 14 were male and 16 were female, with an average age of 53.8 ± 13.3 years and a BMI ranging from 20.76 to 31.14 kg/m². Eighteen participants presented with hepatic lesions, and one target lesion per participant was selected for lesion CNR analysis. Details of lesion types and size ranges are available in the Table S1.

3.2 Comparison of Sequence Scan Times Among Groups

In the diaphragm-unassisted navigation group, as the radial sampling ratio increased from 100% to 180%, the mean scan times were 57.0 ± 13.4 s, 66.0 ± 7.2 s, 76.8 ± 8.5 s, 87.6 ± 9.4 s, and 100.1 ± 14.8 s, respectively. Conversely, in the diaphragm-assisted navigation group, the corresponding scan times were notably longer: 185.4 ± 66.5 s, 189.5 ± 36.2 s, 211.9 ± 56.2 s, 249.0 ± 59.4 s, and 271.4 ± 93.1 s (Table 1). For any given radial sampling ratio, scan times in the diaphragm-assisted group consistently exceeded those in the diaphragm-unassisted group. Within each navigation condition, scan times increased approximately with higher radial sampling ratios.

3.3 Results of Objective Image Quality Assessment

The interobserver agreement for the objective quantitative metrics was excellent, with an ICC range of 0.846 to 0.971. A two-way repeated-measures ANOVA revealed that both diaphragmatic navigation status and radial sampling fraction had significant main effects on liver SNR, background noise SD, and lesion CNR (all $P < 0.001$). The interaction between these factors significantly affected SNR and lesion CNR ($P = 0.027$ and $P < 0.001$, respectively). However, the interaction effect on background noise SD was not statistically significant ($P = 0.086$) (Table 2).

The differences in objective evaluation metrics among the ten sequences were statistically significant (all $P < 0.001$). Descriptive statistics revealed that in the diaphragm-navigation–absent group, the liver SNR increased from 77.54 ± 26.73 to 127.72 ± 74.00 as the radial sampling ratio rose. In contrast, the diaphragm-navigation–added group saw an increase from 101.58 ± 34.31 to 175.15 ± 83.50. The background noise standard deviation (SD) decreased from 10.42 ± 3.81 to 6.78 ± 2.65 in the diaphragm-navigation–absent group and from 8.60 ± 3.16 to 4.99 ± 2.05 in the diaphragm-navigation–added group. Lesion contrast-to-noise ratio (CNR) improved from 25.56 ± 18.26

to 41.02 ± 21.64 in the diaphragm-navigation–absent group and from 52.42 ± 23.41 to 103.01 ± 54.81 in the diaphragm-navigation–added group (Table 3). At the same radial sampling ratio, the diaphragm-navigation–added group exhibited higher SNR and lesion CNR, alongside lower background noise SD, compared to the diaphragm-navigation–absent group (Fig. 1).

3.4 Results of Subjective Image Quality Assessment

The interobserver agreement between the two readers was strong, with a weighted Kappa ranging from 0.824 to 0.911. A comprehensive comparison across the 10 sequence groups revealed statistically significant differences in all seven subjective assessment metrics (all $P < 0.001$) (Table 4). Notably, at identical radial sampling proportions, the diaphragm-navigated groups consistently outperformed the non-navigated groups in all subjective measures. As the radial sampling Percentageincreased, there was a marked improvement in intrahepatic vessel conspicuity, lesion conspicuity, and overall image quality, alongside a reduction in streak artifacts. In the non-diaphragm-navigated groups, the median scores for these metrics ranged from 2.00 to 3.00, whereas in the diaphragm-navigated groups, the medians rose to between 3.00 and 5.00 (Table 4).

Pairwise comparisons revealed that the 140% navigation group shared the same letter designation as the 160% and 180% navigation groups regarding liver edge sharpness, intrahepatic vascular clarity, lesion conspicuity, fat suppression efficacy, and overall image quality. This indicates no statistically significant differences among these groups. In contrast, the 140% navigation group was assigned different letters from the lower sampling-ratio groups and most non-navigation groups, highlighting a notable improvement in image quality (Fig. 2). Interestingly, the mean scan time for the 140% navigation group was 211.9 seconds, almost a minute shorter than the 271.4 seconds recorded for the 180% navigation group.

3.5 Representative Image Results

Figures 3, 4, and 5 display representative images. At identical radial sampling ratios, incorporating the navigator sequence enhanced the clarity of liver margins and intrahepatic vessels, while also reducing streak artifacts and motion blurring. As the radial sampling ratio increased from 100% to 140%, image sharpness improved significantly. However, there were minimal visual differences among the 140%, 160%, and 180% navigator groups. At the lesion level, the navigator enhanced the delineation of lesion borders, with the 140% navigator group already providing relatively clear visualization of lesion margins.

4 Discussion

This study systematically assessed the impact of diaphragmatic navigator gating and radial sampling fraction on the image quality and scanning efficiency of free-breathing liver 3D VANE MRI. The findings indicate that diaphragmatic navigation enhances both subjective scores and objective metrics, including SNR and CNR. Increasing the radial sampling fraction further diminishes background noise and improves image quality, albeit with an extended scan duration. In this study, a 140% radial sampling fraction, when paired with diaphragmatic navigation, offered an optimal balance between image quality and scanning efficiency, suggesting it as a potentially ideal parameter choice.

4.1 The Value of Diaphragmatic Navigation

Diaphragmatic navigation enhances image quality through an effective motion-compensation mechanism. During free breathing, the liver moves with respiration, often resulting in blurred edges[21], poor vascular depiction, and

diminished lesion contrast. By limiting data acquisition to stable respiratory phases, diaphragmatic navigation reduces misregistration and motion blur, thereby enhancing edge sharpness, detail depiction, and lesion visibility.Previous studies support the use of navigators or respiratory-triggering strategies to improve image quality in free-breathing liver MRI. For instance, Reithmeier et al [22]. demonstrated that navigator-triggered acquisition in liver DWI offers higher lesion conspicuity and contrast-to-noise ratio (CNR) compared to free breathing. Similarly, Ichikawa et al [20]. found that combining stack-of-stars with navigator echoes surpassed non-navigator protocols in image quality, hepatic edge sharpness, and vascular clarity during non-breath-hold hepatobiliary-phase imaging.

In our study, using the same radial sampling fraction, the diaphragmatic-navigated group showed superior overall performance. This aligns with previous findings, underscoring the importance of maintaining a stable respiratory phase to enhance image quality in free-breathing liver MRI.

4.2 Marginal Effects of Increasing Radial Sampling Proportion

Enhancing the Percentageof radial sampling improves the completeness of k-space coverage. The stack-of-stars trajectory, which repeatedly samples the k-space centre during acquisition, is more resilient to respiratory motion compared to conventional Cartesian sampling. However, insufficient radial sampling can still result in stripe artefacts, image non-uniformity, and loss of detail [23]. In this study, increasing the Percentageof radial sampling led to improved overall subjective scores, higher SNR and lesion CNR, and a reduction in the standard deviation of background noise. These findings suggest that more complete k-space filling mitigates undersampling artefacts and enhances signal stability.

The enhancement in image quality does not increase linearly with the sampling fraction; instead, it shows diminishing marginal returns. In the absence of navigation, free breathing leads to respiratory phase inconsistencies and periodic liver displacement, which can intensify blurring and streak artifacts [24]. A higher Percentageof radial sampling can mitigate these undersampling and motion-related artifacts through signal averaging. When diaphragm navigation is employed, data acquisition is restricted to a relatively stable respiratory phase, thereby reducing respiration-related misregistration and enhancing data consistency [25]. Consequently, the subjective improvements in image quality from further increases in radial sampling fraction may gradually diminish.

In this study, the addition of diaphragmatic navigation resulted in most subjective metrics stabilising at 140% radial sampling. Increasing the sampling to 160% and 180% improved some objective measures but offered limited subjective benefits and significantly extended scan time. These results align with previous findings that suggest increasing radial percentage can enhance image uniformity and reduce motion-related and streak artifacts. However, they also indicate that once a certain sampling threshold is reached, further improvements in image quality plateau, while scan time continues to rise [19]. Thus, 140% radial sampling with diaphragmatic navigation may represent an optimal balance between image quality and scanning time under the conditions of this study.

4.3 Clinical Implications

Clinically, the use of free-breathing 3D VANE MRI with diaphragmatic navigation minimises the need for patient breath-hold cooperation. In this study, the average scan time for 140% radial sampling with diaphragmatic navigation was around 3.5 minutes. This duration is shorter than that of groups with higher sampling ratios, yet most subjective image quality metrics were comparable to those of the 160% and 180% groups. Consequently, this parameter combination could effectively balance image quality and scanning efficiency in free-breathing liver MRI.

5 Limitations

This study has several limitations. Firstly, it was conducted at a single centre using a specific vendor platform and involved a relatively small sample size. Consequently, the findings need validation through multicentre studies, utilising devices from various manufacturers and employing different reconstruction strategies. Secondly, the lesion CNR analysis included a limited number of lesions, predominantly cystic in nature. Therefore, the applicability of these findings to solid or malignant hepatic lesions remains uncertain. Thirdly, the study primarily concentrated on image quality and scanning efficiency, without systematically assessing lesion detectability, diagnostic accuracy, or patient tolerability. Lastly, only five distinct radial sampling ratio levels were tested, which means it cannot be definitively concluded that 140% is the optimal value across all parameter conditions.

6 Conclusions

The quality of free-breathing liver 3D VANE MRI images is significantly influenced by diaphragmatic navigation and the radial sampling ratio. Diaphragmatic navigation effectively reduces blurring caused by respiratory motion, enhancing both signal-to-noise ratio (SNR) and lesion contrast-to-noise ratio (CNR). Meanwhile, increasing the radial sampling ratio diminishes background noise and reduces undersampling artifacts, albeit at the cost of longer scan times. In this study, a 140% radial sampling ratio combined with diaphragmatic navigation offered an optimal balance between image quality and acquisition efficiency. This parameter set may be preferable, though further validation is needed in larger cohorts, multicentre studies, and across various scanner platforms.

Declarations

Author Contribution

The authors listed below have made significant contributions to the intellectual content of the paper across various sections, as detailed below. Conception and design were led by Yajie Liu, Yongkun Kang, Ruirui Yang, Boyun Yan, and Huicong Shen. Acquisition of data was performed by Ruirui Yang, Boyun Yan, Huicong Shen, Zhaoying Liu, and Jiuming Fu. Analysis and interpretation of data were conducted by Ruirui Yang, Boyun Yan, and Huicong Shen. The drafting of the manuscript was handled by Ruirui Yang. Yajie Liu and Yongkun Kang critically revised the manuscript for important intellectual content. Statistical analysis was performed by Ruirui Yang and Boyun Yan. Administrative, technical, or material support was provided by Zhaoying Liu and Jiuming Fu. Supervision of the project was carried out by Yajie Liu and Yongkun Kang. Other contributions: None specified. All authors reviewed and approved the final version of the manuscript.

Data Availability

The datasets generated and/or analysed during the current study are not publicly available due to patient privacy and ethical restrictions, but may be made available from the corresponding author upon reasonable request and with permission from the relevant institutional authorities.

References

1. Patel R, Aslam A, Parikh ND, et al (2023) Updates on LI-RADS Treatment Response Criteria for Hepatocellular Carcinoma: Focusing on MRI. Magnetic Resonance Imaging 57:1641–1654. https://doi.org/10.1002/jmri.28659

2. Cannella R, Sartoris R, Grégory J, et al (2021) Quantitative magnetic resonance imaging for focal liver lesions: Bridging the gap between research and clinical practice. The British Journal of Radiology 94:20210220. https://doi.org/10.1259/bjr.20210220
3. Fang ZR, Chen QY, YE Ling, et al (2024) Application of compressed sensing combined with parallel acqusition technique of breath-holding 3D LAVA FLEX sequence in rapid magnetic resonance imaging of liver. Chin J Magn Reson Imaging 15:155–161. https://doi.org/10.12015/issn.1674-8034.2024.02.023
4. Kolokythas O, Yaman Akcicek E, Akcicek H, et al (2024) T1-weighted motion mitigation in abdominal MRI: Technical principles, clinical applications, current limitations, and future prospects. RadioGraphics 44:e230173. https://doi.org/10.1148/rg.230173
5. Yang R, Shen H, Yan B, et al (2026) Achieving free-breathing liver magnetic resonance imaging by combining compressed sensing with the number of excitations. Abdom Radiol. https://doi.org/10.1007/s00261-026-05406-3
6. Zhao D, Kong X, Yang K, et al (2025) Deep learning-enhanced super-resolution diffusion-weighted liver MRI: Improved image quality, diagnostic performance, and acceleration. Insights Imaging 16:273. https://doi.org/10.1186/s13244-025-02150-y
7. Parkes MJ, Green S, Stevens AM, Clutton-Brock TH (2014) Assessing and ensuring patient safety during breath-holding for radiotherapy. BJR 87:20140454. https://doi.org/10.1259/bjr.20140454
8. Altinkaya N, Koc Z, Ulusan S, et al (2011) Effects of respiratory manoeuvres on hepatic vein doppler waveform and flow velocities in a healthy population. European Journal of Radiology 79:60–63. https://doi.org/10.1016/j.ejrad.2010.01.011
9. Lin X, Dai L, Yang Q, et al (2023) Free-breathing and instantaneous abdominal T2 mapping via single-shot multiple overlapping-echo acquisition and deep learning reconstruction. Eur Radiol 33:4938–4948. https://doi.org/10.1007/s00330-023-09417-2
10. Lee Y, Yoon S, Park SH, Nickel MD (2024) Advanced abdominal MRI techniques and problem-solving strategies. J Korean Soc Radiol 85:345. https://doi.org/10.3348/jksr.2023.0067
11. Ren Z, Zhang X, Duan H, Nan Y (2025) Improving image quality by comparing two chest MRI sequences: Free-breathing T1-weighted star-VIBE and breath-holding T1-weighted 3D VIBE dixon. Radiologie 65:52–58. https://doi.org/10.1007/s00117-025-01445-x
12. Browne LP, Malone LJ, Englund EK, et al (2022) Free-breathing magnetic resonance imaging with radial k-space sampling for neonates and infants to reduce anesthesia. Pediatr Radiol 52:1326–1337. https://doi.org/10.1007/s00247-022-05298-7
13. Kaltenbach B, Roman A, Polkowski C, et al (2017) Free-breathing dynamic liver examination using a radial 3D T1-weighted gradient echo sequence with moderate undersampling for patients with limited breath-holding capacity. European Journal of Radiology 86:26–32. https://doi.org/10.1016/j.ejrad.2016.11.003
14. Kang M, Otazo R, Behr G, Kee Y (2025) 5D image reconstruction exploiting space-motion-echo sparsity for accelerated free-breathing quantitative liver MRI. Medical Image Analysis 102:103532. https://doi.org/10.1016/j.media.2025.103532
15. Vasanawala SS, Iwadate Y, Church DG, et al (2010) Navigated abdominal T1-W MRI permits free-breathing image acquisition with less motion artifact. Pediatr Radiol 40:340–344. https://doi.org/10.1007/s00247-009-1502-4
16. Feng L (2022) Golden-Angle Radial MRI: Basics, Advances, and Applications. Magnetic Resonance Imaging 56:45–62. https://doi.org/10.1002/jmri.28187

17. Gao C, Ghodrati V, Shih S-F, et al (2023) Undersampling artifact reduction for free-breathing 3D stack-of-radial MRI based on a deep adversarial learning network. Magnetic Resonance Imaging 95:70–79. https://doi.org/10.1016/j.mri.2022.10.010
18. Xue Y, Yu J, Kang HS, et al (2012) Automatic coil selection for streak artifact reduction in radial MRI. Magnetic Resonance in Med 67:470–476. https://doi.org/10.1002/mrm.23023
19. Shin H, Jeong J, Hong S, et al (2019) A study on the image comparison of 3D VANE XD technique in T1 weighted images of liver MRI with free breathing technique as the radial percentage parameter changes. JSMRT 29:17–22. https://doi.org/10.31159/ksmrt.2019.29.1.17
20. Pan J, Shao X, Liu H, et al (2023) Image quality optimization: Dynamic contrast-enhanced MRI of the abdomen at 3T using a continuously acquired radial golden-angle compressed sensing acquisition. Abdom Radiol 49:399–405. https://doi.org/10.1007/s00261-023-04035-4
21. Nepal P, Bagga B, Feng L, Chandarana H (2023) Respiratory motion management in abdominal MRI: *radiology* in training. Radiology 306:47–53. https://doi.org/10.1148/radiol.220448
22. Reithmeier B, Laun FB, Führes T, et al (2024) Relevance of lesion size in navigator-triggered and free-breathing diffusion-weighted liver MRI. Eur Radiol 35:2106–2115. https://doi.org/10.1007/s00330-024-11063-1
23. Feng L, Axel L, Chandarana H, et al (2016) XD-GRASP: Golden-angle radial MRI with reconstruction of extra motion-state dimensions using compressed sensing. Magnetic Resonance in Med 75:775–788. https://doi.org/10.1002/mrm.25665
24. Chiu F-M, Chai J-W, Fang Y-T, et al (2025) Reduction of respiratory motion artifacts in free-breathing abdominal MRI using strategic averaging of reassembled k-space data with self-modeled respiratory state sorting. Physica Medica 139:105185. https://doi.org/10.1016/j.ejmp.2025.105185
25. Bouchaibi SE, Coenegrachts K, Bali MA, et al (2015) Focal liver lesions detection: Comparison of respiratory-triggering, triggering and tracking navigator and tracking-only navigator in diffusion-weighted imaging. European Journal of Radiology 84:1857–1865. https://doi.org/10.1016/j.ejrad.2015.06.018

Tables

Table 1
presents various parameter combinations and scanning durations for 3D VANE MRI used in free-breathing liver examinations.

Group	Radial percentage (%)	Navigator status	Scan time (s)	Approximate scan time
1	100	off	57.0 ± 13.4	0 min 57 s
2	120	off	66.0 ± 7.2	1 min 06 s
3	140	off	76.8 ± 8.5	1 min 17 s
4	160	off	87.6 ± 9.4	1 min 28 s
5	180	off	100.1 ± 14.8	1 min 40 s
6	100	on	185.4 ± 66.5	3 min 05 s
7	120	on	189.5 ± 36.2	3 min 10 s
8	140	on	211.9 ± 56.2	3 min 32 s
9	160	on	249.0 ± 59.4	4 min 09 s
10	180	on	271.4 ± 93.1	4 min 31 s

Note

The term "Radial percentage" refers to the radial sampling ratio. In the context of Navigator status, "off" signifies the absence of diaphragm navigation, while "on" indicates its utilisation. "Scan time" is presented as the mean ± standard deviation of the actual scanning duration, measured in seconds. The approximate scan time, rounded to the nearest minute and second, serves solely for intuitive display purposes.

Table 2
Comparison results of subjective scores among multiple groups of different groups

Outcome	Effect	$F(df_1, df_2)$	Partial η^2	P value
SNR	Navigator	50.088 (1, 29)	0.633	< 0.001
SNR	Radial	30.278 (4, 116)	0.511	< 0.001
SNR	Navigator × Radial	3.134 (4, 116)	0.098	0.027
SD	Navigator	22.589 (1, 29)	0.438	< 0.001
SD	Radial	40.511 (4, 116)	0.583	< 0.001
SD	Navigator × Radial	2.548 (4, 116)	0.081	0.086
CNR	Navigator	41.782 (1, 17)	0.711	< 0.001
CNR	Radial	27.358(4, 68)	0.617	< 0.001
CNR	Navigator × Radial	8.632(4, 68)	0.337	< 0.001

Note:This study defined two factors: diaphragm navigation (Navigator) and radial sampling ratio (Radial), with their interaction denoted as Navigator × Radial. Evaluated quantitative parameters included liver signal-to-noise ratio (SNR), background noise standard deviation (SD), and lesion contrast-to-noise ratio (CNR).The sphericity

assumption was tested for the radial sampling ratio and its interaction with navigator status. Greenhouse-Geisser correction was adopted when sphericity was violated, with corrected degrees of freedom and p-values presented. Partial η^2 was calculated for effect size.

Table 3
Comparison results of objective scores among multiple groups of different groups

Group	Liver SNR	Background SD	Lesion CNR
100%	77.54 ± 26.73	10.42 ± 3.81	25.561 ± 18.264
120%	89.82 ± 37.30	9.59 ± 3.62	28.216 ± 19.005
140%	102.39 ± 45.56	8.18 ± 3.21	36.077 ± 25.528
160%	110.85 ± 56.60	7.39 ± 3.02	40.518 ± 24.470
180%	127.72 ± 74.00	6.78 ± 2.65	41.019 ± 21.638
100% with navigation	101.58 ± 34.31	8.60 ± 3.16	52.420 ± 23.414
120% with navigation	118.57 ± 51.95	7.47 ± 2.87	65.194 ± 32.044
140% with navigation	143.49 ± 79.36	6.55 ± 2.77	79.791 ± 36.467
160% with navigation	149.95 ± 75.77	6.74 ± 2.29	79.282 ± 35.553
180% with navigation	175.15 ± 83.50	4.99 ± 2.05	103.007 ± 54.813
P value	< 0.001	< 0.001	< 0.001

Note

Objective scoring data are presented as mean ± standard deviation. The liver signal-to-noise ratio (SNR) and the standard deviation (SD) of background noise were derived from a sample of 30 subjects, whereas the lesion contrast-to-noise ratio (CNR) was calculated from 18 lesions. The *P* value indicates the overall comparison result across 10 groups of sequences.

Table 4
Intergroup comparison of subjective image quality scores across different groups

Group	Liver margin sharpness	Intrahepatic vessel visibility	Streak artifacts	Lesion conspicuity	Overall image quality	Fat suppression quality	Pancreatic structure visibility
100%	4.00(4.00, 4.00)	2.00(2.00, 3.00)	2.00(2.00, 2.25)	2.00(2.00, 2.00)	2.00(2.00, 3.00)	2.00(2.00, 2.00)	1.00(1.00, 2.00)
120%	4.00(4.00, 4.00)	3.00(2.00, 3.00)	2.00(2.00, 3.00)	2.00(2.00, 3.00)	2.00(2.00, 3.00)	2.00(2.00, 2.00)	1.00(1.00, 2.00)
140%	4.00(4.00, 4.00)	3.00(3.00, 3.00)	3.00(2.00, 3.00)	3.00(2.25, 3.00)	3.00(2.75, 3.00)	2.00(2.00, 2.00)	2.00(2.00, 2.00)
160%	4.00(4.00, 4.00)	3.00(3.00, 4.00)	3.00(3.00, 4.00)	3.00(3.00, 3.00)	3.00(3.00, 4.00)	2.00(2.00, 2.00)	2.00(2.00, 3.00)
180%	4.00(4.00, 4.00)	3.00(3.00, 4.00)	3.00(3.00, 4.00)	3.00(3.00, 3.00)	3.00(3.00, 4.00)	2.00(2.00, 2.00)	2.00(2.00, 3.00)
100% with navigation	5.00(5.00, 5.00)	4.00(4.00, 4.00)	3.00(2.00, 3.00)	4.00(4.00, 4.00)	4.00(4.00, 4.00)	4.00(4.00, 5.00)	3.00(3.00, 3.00)
120% with navigation	5.00(5.00, 5.00)	4.00(4.00, 5.00)	3.00(3.00, 4.00)	4.00(4.00, 4.00)	4.00(4.00, 4.00)	4.00(4.00, 5.00)	3.00(3.00, 4.00)
140% with navigation	5.00(5.00, 5.00)	5.00(5.00, 5.00)	4.00(3.00, 4.00)	5.00(4.00, 5.00)	5.00(5.00, 5.00)	4.00(4.00, 5.00)	4.00(4.00, 4.00)
160% with navigation	5.00(5.00, 5.00)	5.00(5.00, 5.00)	4.00(4.00, 4.00)	5.00(4.00, 5.00)	5.00(5.00, 5.00)	4.00(4.00, 5.00)	4.00(4.00, 4.00)
180% with navigation	5.00(5.00, 5.00)	5.00(5.00, 5.00)	4.00(4.00, 4.00)	5.00(4.00, 5.00)	5.00(5.00, 5.00)	4.00(4.00, 5.00)	4.00(4.00, 4.00)
P value	< 0.001	< 0.001	< 0.001	< 0.001	< 0.001	< 0.001	< 0.001

Note

Subjective scores are presented as median (Q1, Q3). *P* values represent overall comparisons across the 10 sequences. Lesion conspicuity was evaluated in the 18 subjects with hepatic lesions, whereas all other subjective metrics were assessed in all 30 subjects.

Figures

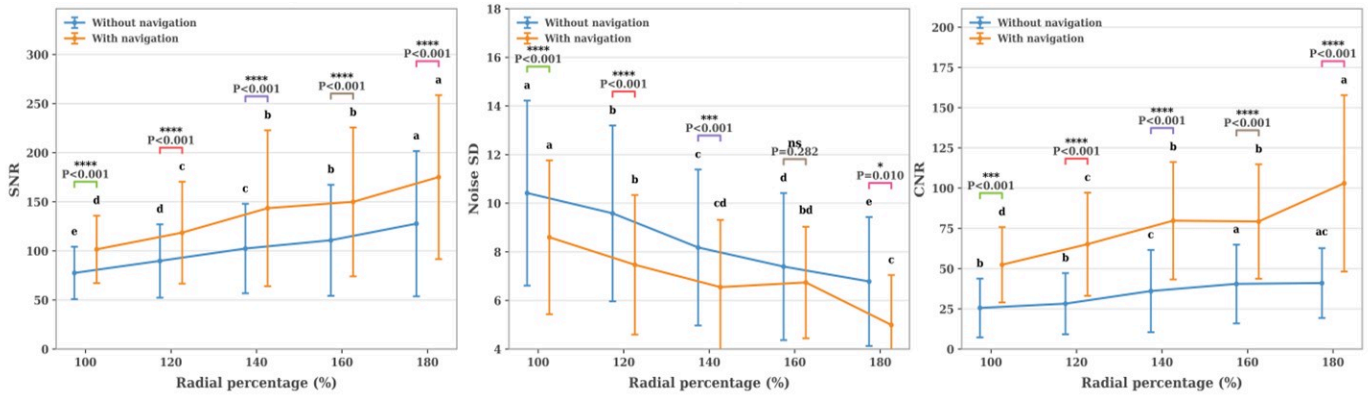


Figure 1

presents the results of the objective image evaluation.

Note: Data are shown as mean ± standard deviation (SD). Each data point represents the average value for a group, with error bars indicating the SD. Asterisks denote the results of pairwise comparisons between the diaphragmatic navigation group and the non-diaphragmatic navigation group at the same radial sampling ratio: 'ns' signifies no statistically significant difference, while *P< 0.05, **P < 0.01, ***P < 0.001, and ****P < 0.0001 indicate increasing levels of statistical significance. Letter groupings from pairwise comparisons of 10 sequence groups (following Holm correction) are also shown. Groups without common letters differ significantly, whereas those with common letters do not.

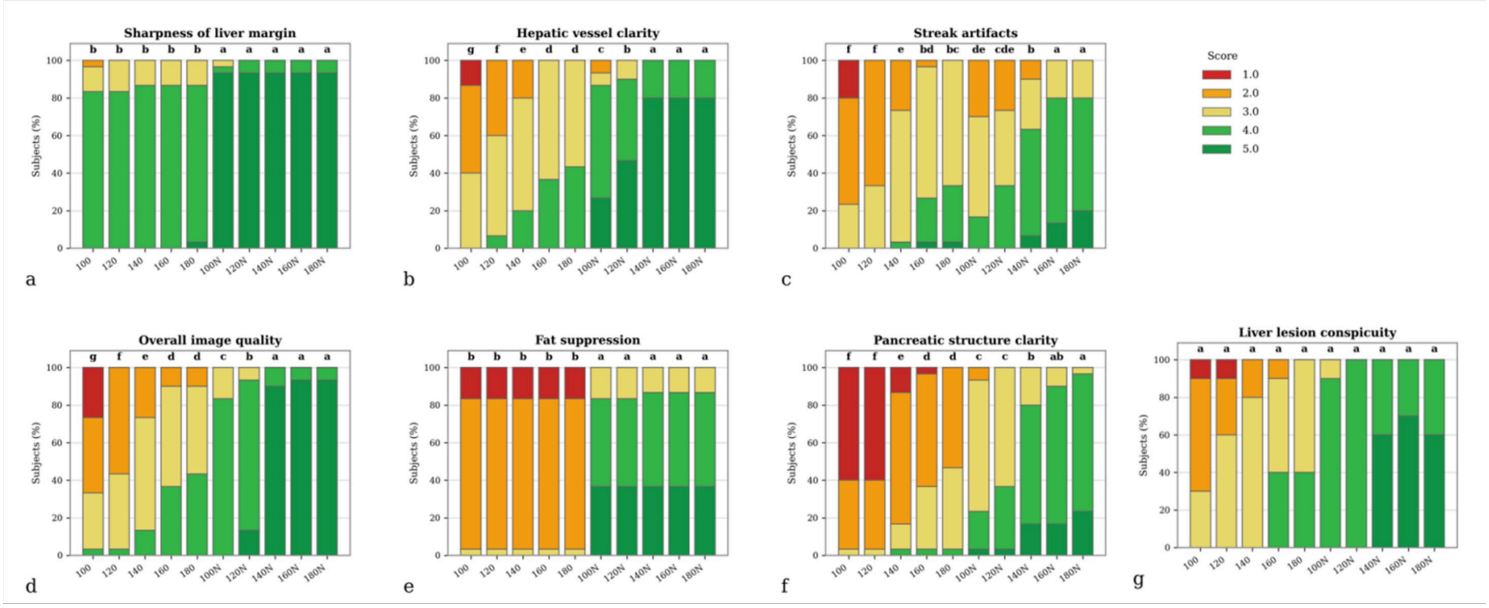


Figure 2

presents the results of the subjective image assessment.

Note: The stacked bar chart illustrates the composition ratio for each score grade, ranging from 1 to 5 points. An overall comparison was conducted using the Friedman test, while pairwise comparisons were performed using the Wilcoxon paired signed rank test, with corrections applied by Holm. Columns marked with different letters indicate statistically significant differences between groups, whereas identical letters denote no significant difference. 'N' denotes the diaphragmatic navigation group.

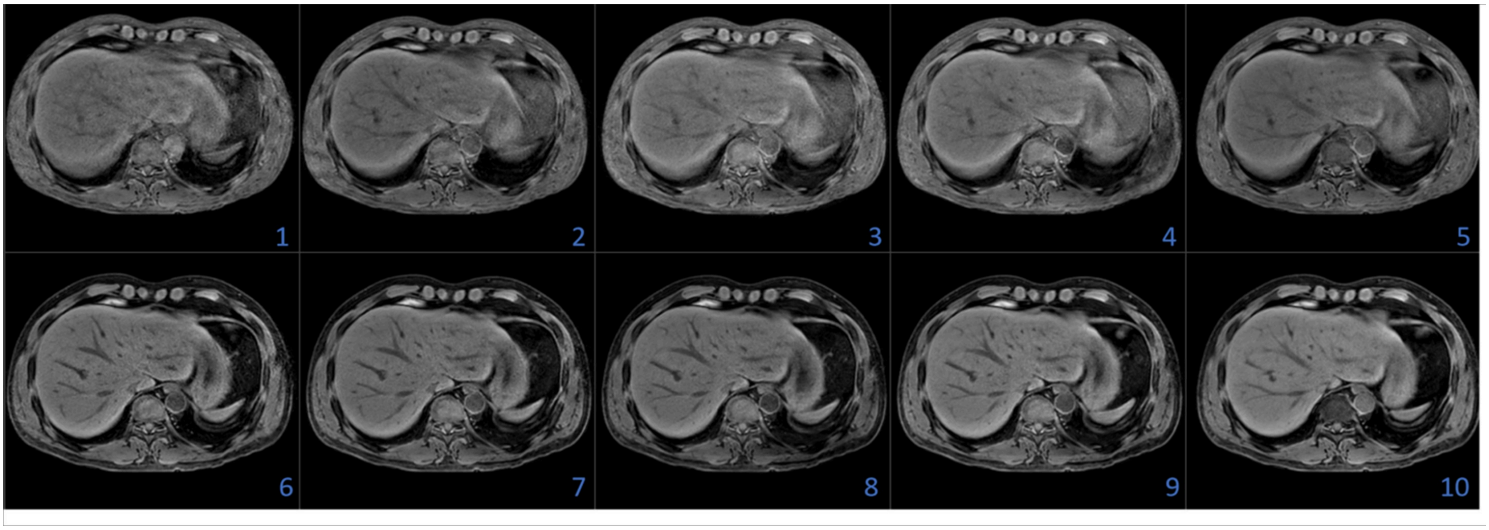


Figure 3

depicts a 48-year-old male with a BMI of 22.85 kg/m², illustrating the hepatic vascular laye

Note: In the figure, sequences 1 to 5 represent those without diaphragm navigation, with radial sampling ratios of 100%, 120%, 140%, 160%, and 180%, respectively. Sequences 6 to 10 depict those with diaphragm navigation, also with radial sampling ratios of 100%, 120%, 140%, 160%, and 180%, respectively.

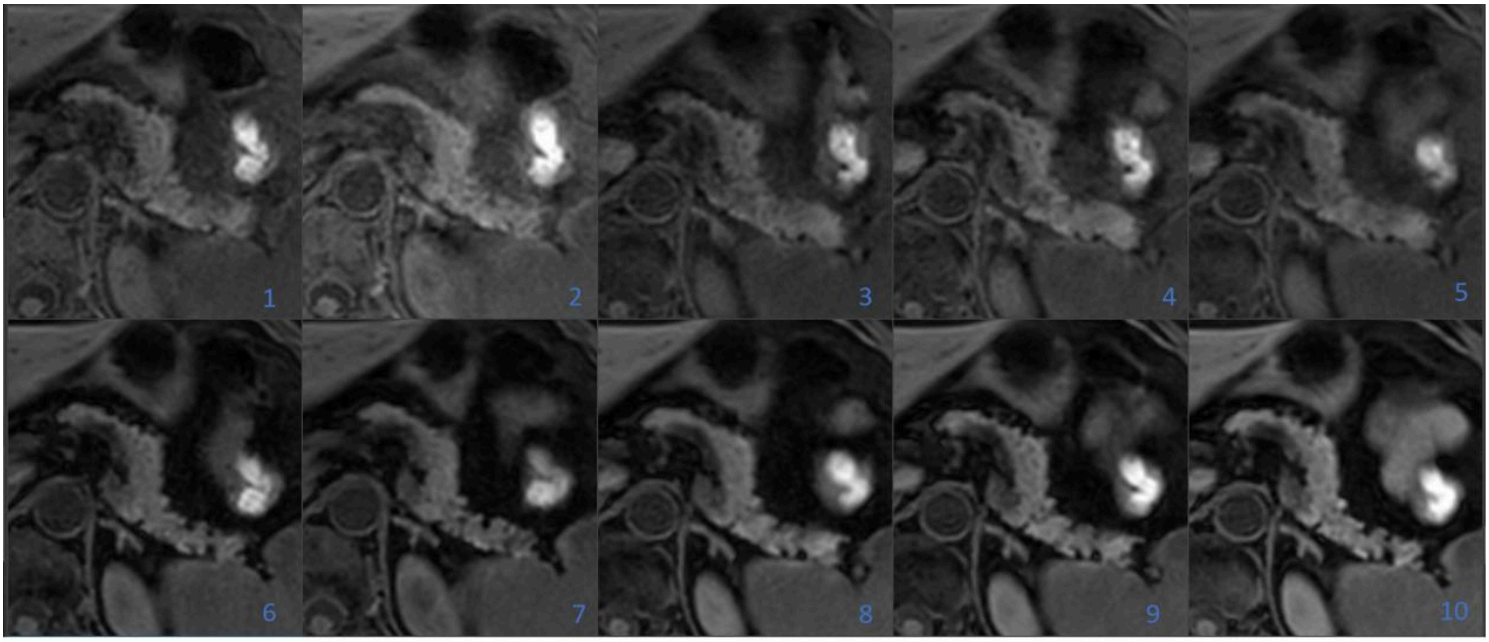


Figure 4

depicts a 56-year-old woman with a BMI of 22.03 kg/m², illustrating the image at the pancreatic level.

Note: The numbers correspond directly to those in Figure 3.

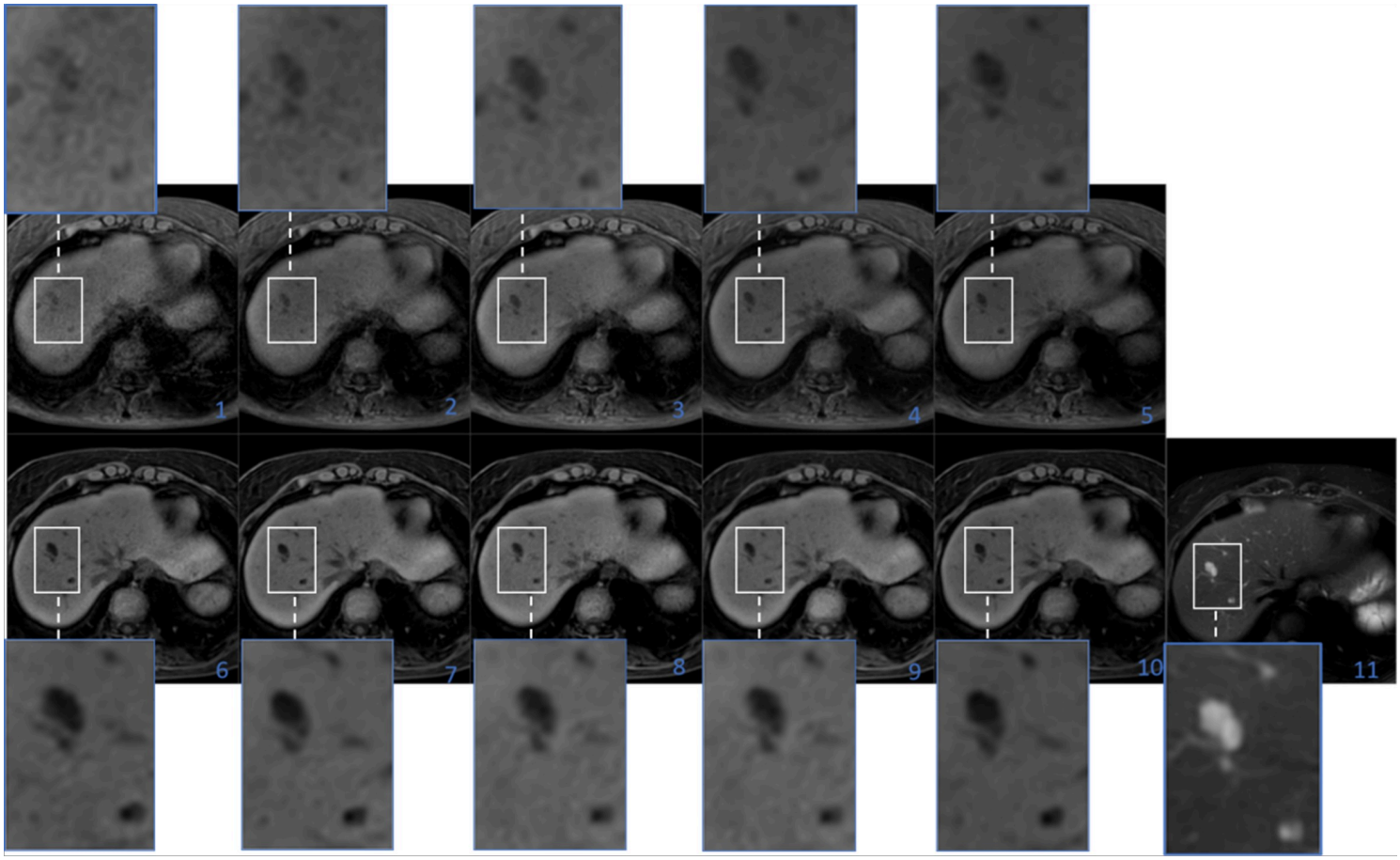


Figure 5

depicts a 59-year-old female with a BMI of 21.77 kg/m², illustrating the extent of liver cysts.

Note:The numbers 1 to 10 correspond directly to those in Figure3, with 11 denoting T2WI.

Supplementary Files

This is a list of supplementary files associated with this preprint. Click to download.

- Attachment.docx